*Cellular and Molecular Bioengineering*, Vol. 16, No. 2, April 2023 *(© 2023)* pp. 143–157
https://doi.org/10.1007/s12195-022-00758-4

*Original Article*

# Investigation of the Therapeutic Effects of Palbociclib Conjugated Magnetic Nanoparticles on Different Types of Breast Cancer Cell Lines

Maryam Parsian,[1] Pelin Mutlu,[2] Negar Taghavi Pourianazar,[3] Serap Yalcin Azarkan,[4] and Ufuk Gunduz[1,5]

[1]Department of Biotechnology, Middle East Technical University, Ankara, Turkey; [2]Department of Biotechnology, Biotechnology Institute, Ankara University, Ankara, Turkey; [3]Department of Medical Laboratory Techniques, Istanbul Aydin University, Istanbul, Turkey; [4]Department of Molecular Biology and Genetics, Ahi Evran University, Kirsehir, Turkey; and [5]Department of Biological Sciences, Middle East Technical University, Ankara, Turkey

*(Received 1 November 2022; accepted 14 December 2022; published online 7 January 2023)*

Associate Editor Michael R. King oversaw the review of this article.

**Abstract**
*Introduction*—Drug targeting and controlled drug release systems in cancer treatment have many advantages over conventional chemotherapy in terms of limiting systemic toxicity, side effects, and overcoming drug resistance.
*Methods and Results*—In this paper, fabricating nanoscale delivery system composed of magnetic nanoparticles (MNPs) covered with poly-amidoamine (PAMAM) dendrimers and using its advantages were fully used to help the chemotherapeutic drug, Palbociclib, effectively reach tumors, specifically and stay stable in the circulation longer. In order to determine whether conjugate selectivity can be increased for the specific drug type, we have reported different strategies for loading and conjugation of Palbociclib to different generations of magnetic PAMAM dendrimers. The best method leading to the highest amount of Palbociclib conjugation was chosen, and the characterization of the Palbociclib conjugated dendrimeric magnetic nanoparticles (PAL-DcMNPs) were performed. *In vitro* pharmacological activity of the conjugation was demonstrated by measuring the cell viability and lactate dehydrogenase (LHD) release. Obtained results indicated that PAL-DcMNPs treatment of the breast cancer cell lines, leads to an increase in cell toxicity compared to free Palbociclib. The observed effects were more evident for MCF-7 cells than for MDA-MB231 and SKBR3 cells, considering that viability decreased to 30% at 2.5 $\mu$M treatment of PAL-DcMNPs at MCF-7 cells. Finally, in Palbociclib and PAL-DcMNPs treated breast cancer cells, the expression levels of some pro-apoptotic and drug resistance related genes were performed by RT-PCR analysis.
*Conclusion*—Our knowledge indicates that the proposed approach is novel, and it can provide new insight into the development of Palbociclib targeting delivery system for cancer treatment.

**Keywords**—Palbociclib, Palbociclib conjugated magnetic nanoparticles, Targeted delivery, Breast cancer, PAMAM dendrimer.

## INTRODUCTION

In the battle against malignant tumors, chemotherapy is the most common strategy. The inability of anticancer agents to selectively attack tumor cells remains the most significant obstacle to successful chemotherapy.[19] An ideal approach to overcoming these problems is encapsulating the drugs into suitable drug delivery systems. Several smart nanoplatforms are being developed that respond to internal or external stimuli, such as changes in enzymes, pH, hypoxia, redox, magnetic field, temperature, light, and ultrasound.[22]

Iron oxide-based magnetic nanoparticles (MNPs) have gained importance as drug targeting systems due to their simple structure, easy synthesis, and ability to alter their properties for different biological purposes. Such nanoparticles carrying anticancer agents can be condensed in tumor cells with the help of an externally applied magnetic field.[23] However, extensive surface modifications are required to increase the stability of the MNPs in the organism and to protect the nanoparticles from attack by the immune system cells. Organic polymers such as poly-amidoamine (PA-

Address correspondence to Maryam Parsian, Department of Biotechnology, Middle East Technical University, Ankara, Turkey. Electronic mail: smaryamparsian@gmail.com

MAM) dendrimer, polyethylene glycol, chitosan, and aminosilane are widely used polymers for the coating of these nanoparticles.[1, 21, 22]

PAMAM dendrimer is a well-defined, special three-dimensional structure having a multivalent surface and internal cavities that can play an essential role in drug delivery systems.[26] These spherically branched polymers with numerous amine or carboxyl-terminal groups are capable of forming stable complexes with chemotherapeutic drugs and oligonucleotides. The drug conjugated PAMAM dendrimers are pH-sensitive. The polymer rapidly cleaved in acidic pH; however, it was strong enough in physiological conditions. The pH differences between tumors (pH 5.6–6.8) and healthy tissues (pH 7.0–7.4) investigated different microenvironments to release drugs from PAMAM dendrimers. This form of delivery minimizes payload exposure to healthy tissues and maximizes the dose to the site of disease.[10] Palbociclib is a type of targeted drug which is effective in the treatment of different types of tumors, especially against advanced stage or metastatic, hormone receptor-positive (ER+, PR+), HER2 negative breast cancer.[7]

In this study, fabricating Magnetic PAMAM dendrimers (DcMNPs) and using their advantages were fully utilized to help the chemotherapeutic drug, Palbociclib, reach tumors specifically and stay stable during the systemic circulation period in the body. After synthesizing DcMNPs, the drug loading/conjugating on these nanoparticles was examined *via* various methods. A critical issue in dendritic drug delivery systems is achieving a high drug payload. It may be possible that some of the nanocarrier–drug conjugates show less therapeutic activity compared to free drugs due to relatively low drug payload, decoupling immediately after conjugation, or the lack of drug release from the conjugate.[11, 28] Therefore, the main focus of this study was to synthesize DcMNPs conjugates with relatively high Palbociclib loading and increase the conjugations' pharmacological activity inside the cancer cell. The cellular internalization and cytotoxicity effect of these complexes were evaluated in three different breast cancer cell lines, MCF-7 ($ER^+$, $PR^{\pm}$, $HER2^-$), MDA-MB-231($ER^-$, $PR^-$, $HER2^-$), and SKBR-3 ($ER^-$, $PR^-$, $HER2^+$). Finally, the expression patterns of some anti-apoptotic and pro-apoptotic genes were analyzed in Palbociclib conjugated nanoparticles-treated breast cancer cells.

## EXPERIMENTAL SECTION

### *Synthesis of Magnetic PAMAM Dendrimers*

Synthesis of PAMAM dendrimers was previously reported by our group.[22] Different generations of amine and carboxyl end group PAMAM dendrimers were prepared according to the previously described procedure. These synthesized nanoparticles have either positive (with amine end group) or negative (with carboxyl end group) surface charge with suitable size distribution and targetability properties under a magnetic field.[16]

### *Cell Culture*

MCF7, SKBR3, and MDA-MB231 cell lines were used in all experiments. Cells were maintained in RPMI 1640 medium (Lonza, Germany) supplemented with heat-inactivated fetal bovine serum (FBS) (10% (v/v)) (Biochrome, Germany) and gentamicin (1% (v/v)) (Lonza, Germany) in tissue culture flasks (Greiner Bio-one, Germany). Cells were incubated in a Heraeus incubator (Hanau, Germany) at 37 °C supplemented with 5% $CO_2$ and subcultured; when they reached 80% confluency.

### *Cellular Uptake of FITC Modified DcMNPs*

Generation five carboxyl end group (G5.5) DcMNPs were conjugated with fluorescein isothiocyanate (FITC) in ethyl dimethylaminopropyl carbodiimide (EDC) and *N*-hydroxysuccinimide (NHS) solutions to observe cellular uptake into breast cancer cells. The conjugation process was carried out with the surface activation method of EDC/NHS solutions.[2] In this method, 100 $\mu$L FITC (Sigma Aldrich, Germany) (1 mg fluorescein was dissolved in 1 mL DMSO) followed by the addition of 20 mg EDC (Sigma Aldrich, Germany) and 4.6 mg NHS (Sigma Aldrich, Germany), which were dissolved in 2 mL of PBS (pH 5.8) (Sigma Aldrich, Germany) and remained at 4 °C for 2 h.[20] G5.5 DcMNPs (5 mg/mL) was added to the solution and rotated (Biosan Multi RS-60 Rotator) at 100 rpm with 25 s vibration intervals overnight in the light-protected tubes at 4 °C. After incubation time, particles were separated *via* magnetic decantation and washed several times with PBS until the supernatant turned colorless. The obtained FITC-DcMNPs were resuspended in medium to a final concentration of 250 $\mu$g/mL.

### *Confocal Microscopy Analysis*

MCF-7, MDA-MB-231, and SKBR-3 cells, plated at a $5 \times 10^5$ cells/mL density in 6-well plates, were used for uptake studies. After 24 h of culture, when they formed confluent monolayers, each cell monolayer was rinsed thrice and re-incubated with FITC-DcMNPs solution (250 $\mu$g/mL) for 24 h at 37 °C. The experiment was terminated by washing the cell monolayer three times with ice-cold PBS. The resultant cells conjugated with FITC-DcMNPs were visualized by confocal microscopy (Leica Microsystems DM 2500).

### *Flow Cytometry Analysis*

$3.5 \times 10^5$ breast cancer cells were cultured in 2 mL medium in each well of 6-well plates for 24 h in a humidified environment at 37 °C and 5% $CO_2$ until a 70–80% confluence was reached. Then, the medium was removed entirely and replaced with a fresh medium with 250 $\mu$g/mL G5.5 FITC-DcMNPs.[13] The exposure was varied for 1, 2, 4, 6, 8, and 24 h with a constant amount of DcMNPs. After the exposure time, each cell line was prepared for Flow Cytometry analysis separately. Only viable cells were collected for analysis. Cells were washed with PBS and detached with trypsin. After centrifuging, cells were washed and resuspended at PBS. At least 20,000 events per sample were analyzed. Side scattering (SSC) and forward scattering (FSC) were measured by flow cytometry (BD Biosciences, USA).

### *Loading of Palbociclib on DcMNPs*

Loading studies on PAMAM dendrimer-coated magnetic nanoparticles to Palbociclib were carried out in Methanol, PBS (pH 7.2), Tris (pH 7.3), and acetate (pH 5.0) buffers. The Palbociclib and DcMNPs complexes were prepared by mixing equal amounts of the drug solution and different amounts of DcMNPs solution followed by gentle rotating (Biosan Multi rotator RS-60) at 37 °C for 24, 48, and 72 h to ensure the complex formation. The nanoparticles loaded with Palbociclib (Sigma Aldrich, Germany) were separated by magnetic separation (Loading Method I and Loading Method II) and ultracentrifuge methods (Loading Method III). The supernatant was removed and the absorbance was measured at 218 nm with the UV spectrophotometer and HPLC to determine the amount of binding of the drug to the nanoparticles.

### *Synthesis of Magnetic PAMAM–Palbociclib Conjugate*

The linking of the drug to the dendritic chain was done using a covalent method which consists of several steps. 24.40 $\mu$g Palbociclib (50 $\mu$mol) and 150 $\mu$mol EDC were dissolved at 1 ml DMSO (Sigma Aldrich, Germany) and stirred for half an hour at room temperature. 100 $\mu$mol succinic acid (SA) (Sigma Aldrich, Germany) was slowly added to the solution and stirred for 24 h. Excess SA was added to obtain a complete reaction between the drug and SA. Resulting PAL-SA was stirred for 3 h at room temperature in the presence of excess 150 $\mu$mol of EDC. Then 1000 $\mu$g/mL of PAMAM G5.5 was added to the reaction mixture and stirred at room temperature for 2 days (Fig. 1).

The PAL-PAMAM was purified by magnetic separation and the HPLC method was used to measure the amount of drug in the supernatant.[19] The column used in the HPLC study was selected as Agilent C18 (250 mm × 4.6 mm, 5 $\mu$m). A solution containing acetonitrile (300:700, 0.1% TFA) was used as the mobile phase. The determined wavelength is 234 nm/260 nm. The column temperature was set to 40 °C. The flow rate is 1.0 mL/min and the sample size is 10 $\mu$L. HPLC measurements were carried out in METU Central Laboratory.

### *Characterization of Drug Conjugated DcMNPs*

The particle shape and size of the synthesis of nanoparticles loaded with Palbociclib were monitored by electron microscopy (TEM and SEM). In addition, the characterization of DcMNPs loaded with Palbociclib were carried out with potential analyzes of FTIR and zeta-potential. The FT-IR analysis, Transmission Electron Microscopy (F.E.I. Tecnai G2 Spirit BioTwin), SEM, and Zeta-Potential (Malvern NanoZS90) measurements were carried out in METU Central Laboratory.

### *Cell Viability Assay*

MCF-7, SKBR-3, and MDA-MB-231 cells ($1 \times 10^4$ cells/well) were cultured at 50 $\mu$L medium in opaque-walled white multiwell plates for a day. The cells were treated with different concentrations (2.5, 5, 15, 25, 30 and 50 $\mu$M) of Palbociclib and Palbociclib conjugated DcMNPs for 96 h. After incubation time, the plate and its contents were equilibrated to room temperature (22–25 °C) for approximately 30 min. An equal volume of CellTiter-Glo® (Promega, G9681) reagent and cell culture medium was added to each well. The contents were mixed vigorously for 5 min to induce cell lysis. The plate was incubated at room temperature for an additional 25 min to stabilize the luminescent signal. Luminescence was recorded by the SpectraMax iD3 microplate reader.

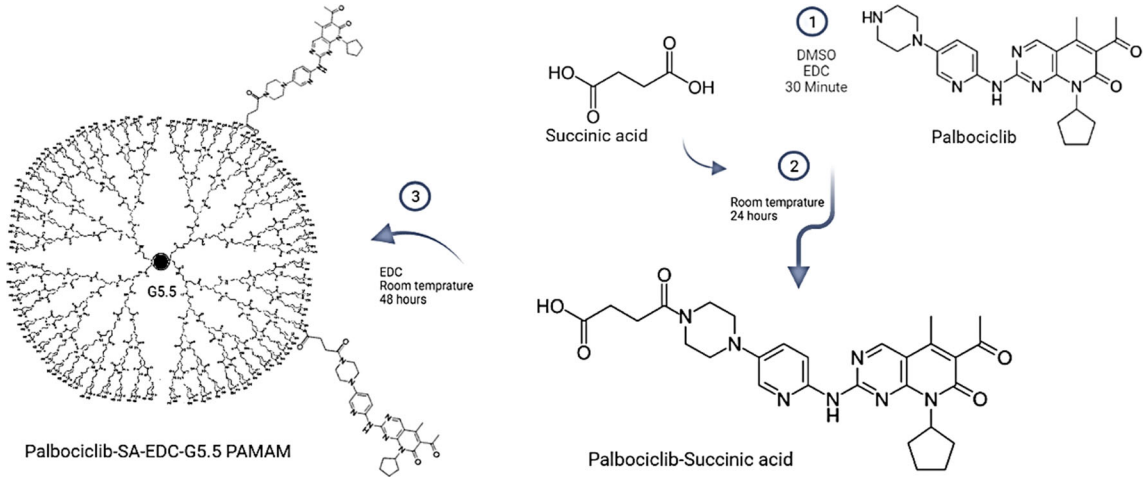


**FIGURE 1. Schematic for Palbociclib–Succinic acid–G5.5 PAMAM conjugation.**

### *LDH Assay*

The breast cancer cells were seeded in 96-well plates ($1 \times 10^4$ cells/well) in 50 $\mu$L of media and then treated with different concentrations (2.5, 5, 15, 25, 30, and 50 $\mu$M) of Palbociclib, PAL-DcMNPs, and bare DcMNPs. The PAL-MNPs were washed twice by PBS to remove the excess amount of drug and DMSO after precipitation by a magnet and resuspended at desired concentration with 5% RPMI 1640 medium. The treated cells were then incubated for 24, 48, 72, and 96 h. Then, non-treated (control) and treated cells (100 $\mu$L) were transferred to separate eppendorf tubes and centrifuged at 1000 rpm for 5 min to remove cell debris. The total amount of released enzyme was determined using a Lactate Dehydrogenase (LDH) Colorimetric Assay kit (Abcam, USA). 5 $\mu$L of all media was added to 45 $\mu$L assay buffer and 50 $\mu$L of reaction mix was added. The absorbance of NADH Standard, positive controls and samples were measured immediately at OD 450 nm (T1) on a microplate-reader (SpectraMax iD3 microplate reader) in a kinetic mode every 2 min for 60 min (T2) at 37 °C protected from light. The LDH activity in the test samples was calculated by using Eq. (1).

$$\text{LDH activity} = \left(\frac{\beta}{\Delta T \times V}\right) \times D = \text{nmol/min/mL} = \text{mU/mL}, \tag{1}$$

where $\beta$ is the amount of NADH in sample well calculated from standard curve (nmol), $\Delta T$ is the reaction time (minutes), $V$ is the original sample volume added into the reaction well (mL) and $D$ is the sample dilution factor.

### *RNA Isolation, cDNA Synthesis, and Real-Time Polymerase Chain Reaction (RT-PCR) Test*

After treatment of the cells with 15 $\mu$M Palbociclib and incubation for 96 h, total RNA was extracted using a high pure RNA isolation kit (Roche, Germany) according to the manufacturer's instructions. Then 1 mg of total RNA was reverse transcribed into cDNA by the high-capacity cDNA reverse transcription kit (Thermofisher, Katalog No: 4368814). Finally, expressions of some essential apoptotic genes such as Bax, Bcl-2, CDH1, MDR1, and mTOR were examined by RT-PCR analysis. The SYBR Green Master Mix (Roche Diagnostics, Switzerland) was used to perform RT-PCR according to the manufacturer's instructions on a LightCycler® 480 instrument (Roche Diagnostics, Switzerland). Fold changes of Bax, Bcl-2, Puma, CDH1, MDR1, and mTOR genes were normalized to the internal control gene GAPDH and calculated for each sample relative to a no-treatment control. Relative fold changes in mRNA levels compared to controls were measured using the $2^{-\Delta\Delta Ct}$ calculations ($\Delta\Delta Ct = \Delta Ct^{\text{treated}} - \Delta Ct^{\text{control}}$).

## RESULTS AND DISCUSSIONS

### *Cellular Uptake of FITC Modified DcMNPs by Confocal Microscopy*

The efficacy of drug-loaded nanoparticles depends on the cellular uptake and the released dose of the drug from the internalized nanoparticles within the cells. In order to determine cellular internalization, FITC conjugated DcMNPs were prepared (Fig. 2). A fluorescent

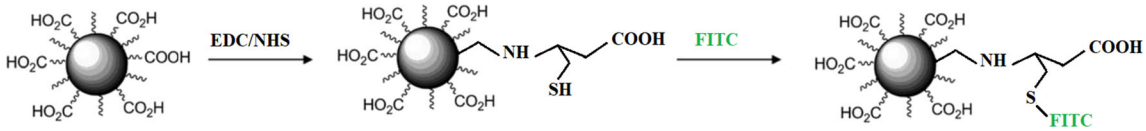


**FIGURE 2. Schematic representation indicating conjugation of G5.5 DcMNPs with FITC in EDC/NHS solutions.**

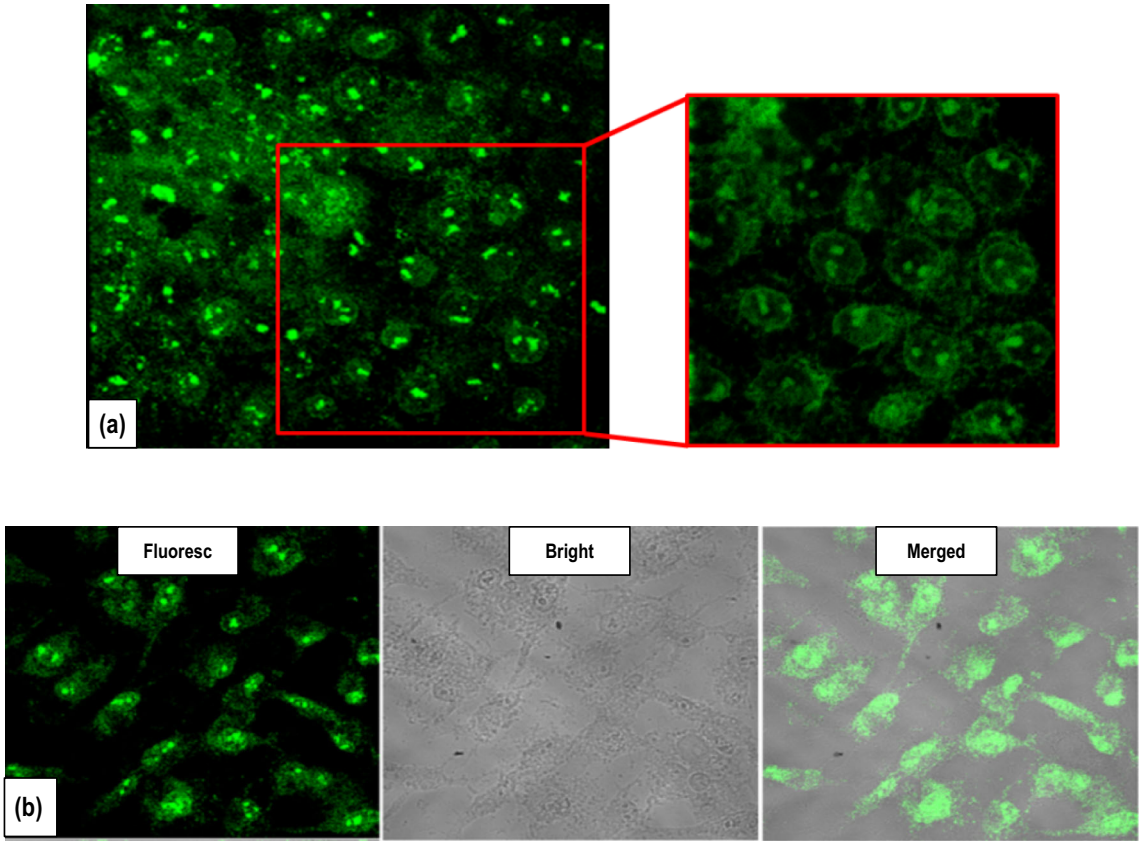


**FIGURE 3. Cellular uptake of FITC-DcMNPs by (a) MCF-7 cells by confocal microscopy (40 X1 and 40 X2 zooms), (b) MDA-MB-231 (40 X1 florescent and bright field).**

dye acts as a probe for DcMNPs and offers a sensitive method to assess intracellular uptake. A similar labeling method was used earlier by Arya et al. to investigate the uptake of chitosan nanoparticles in the human pancreatic cancer cell and embryonic kidney cell lines.[2]

The cellular uptake of FITC conjugated G5.5 DcMNPs were visualized in MCF-7, MDA-MB231, and SKBR-3 breast cancer cell lines by confocal microscopy; (Fig. 3). The reflection of bright green dots inside and around the nucleus indicates the nanoparticles' intracellular localization, expressing the efficient cellular uptake of the particles. In contrast, the bright-field images show no visible particles on the outside or the surface of the cells.

### *Detection of FITC Labeled Magnetic Nanoparticle Internalization in Breast Cancer Cells by Flow Cytometry*

Flow Cytometry analysis is a fast and reliable method to study the uptake of modified nanoparticles by cancer cells. The magnetic nanoparticle-exposed and unexposed cells running in flow Cytometry can be distinguished regarding their light scattering and fluorescence signals. The side scattering correlates with the internal granularity of the cells and provides information about the cellular effects after nanoparticle internalization.[13]

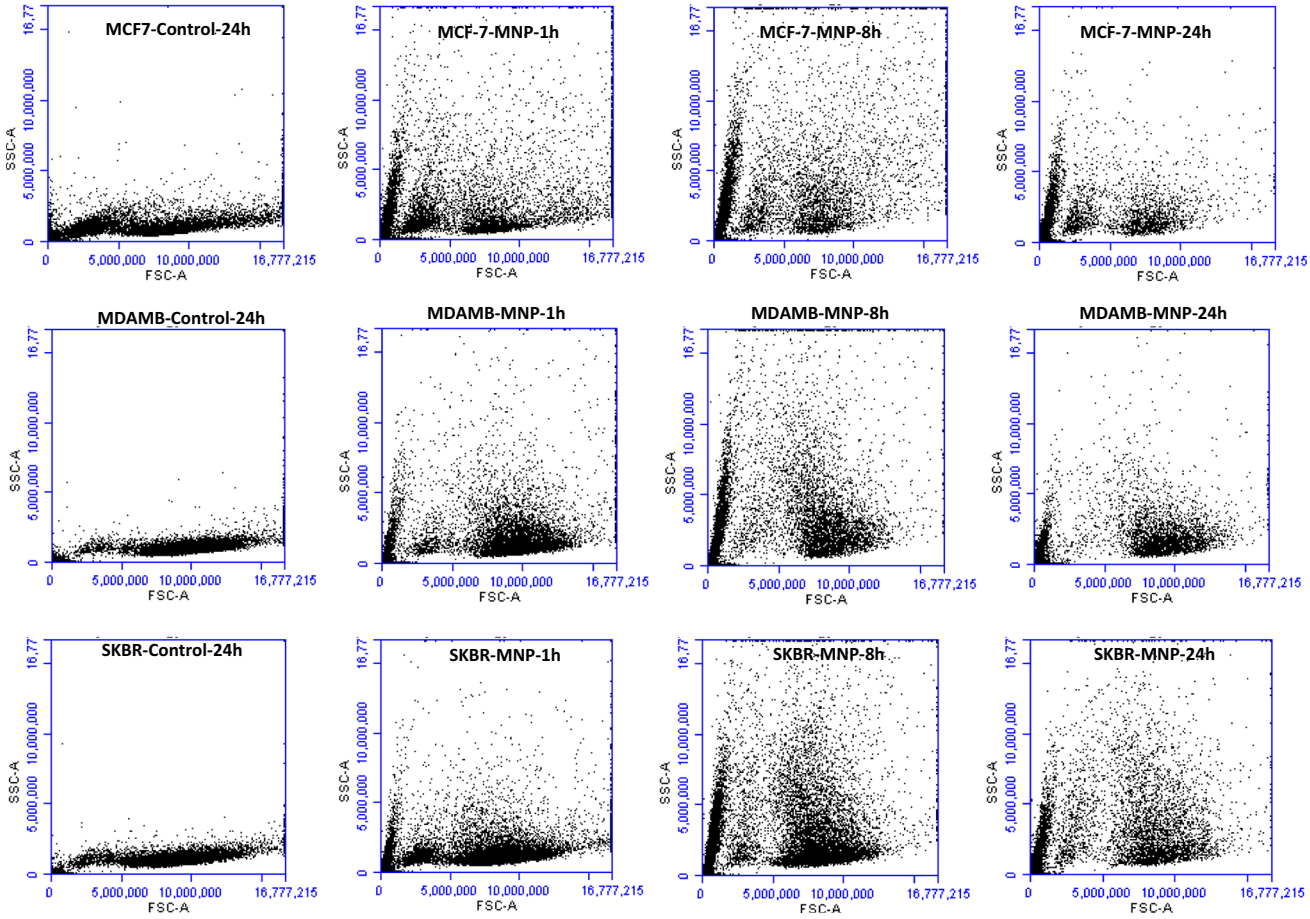


**FIGURE 4. Density plot of SSC and FSC signals of MCF-7, MDA-MB-231, and SKBR-3 cells. Cells were incubated with 250 μg/mL DcMNPs for 24 h.**

As shown in Fig. 4, significant side scattering signals (SSC) changes were displayed in DcMNPs treated cells compared to the control cells. The cytotoxic effects of empty DcMNPs up to 250 μg/mL concentration were evaluated previously by our group.[22] Bare nanoparticles showed no significant cytotoxicity on MCF-7, SKBR-3, and MDA-MB-231 cells. Treatment with constant FITC-DcMNPs concentrations (250 μg/mL) for all cell types showed an increasing time dependence on SSC signals. The exposure was carried out for 1, 2, 4, 6, 8, and 24 h with a constant amount of DcMNPs. All cell lines show the highest uptake efficiency within 24 h of incubation regarding uptake kinetics.

All cell lines show an extremely high uptake rate during the first eight hours of incubation. Between one and eight hours of incubation, the signal intensity was increased, and between eight and 24 h, the signal intensity decreased slightly at MCF-7 and MDA-MB231 cell lines. A redistribution of the nanoparticles during cell division might explain the decrease in scattering after 24 h. Jochum et al. showed the same uptake kinetic for FITC-TiO2 nanoparticles at A549 and NIH/3T3 cell lines.[13]

The decrease of scattering intensity under 2,500,000 signals in all cell lines demonstrated the time-depending internalization of nanoparticles. MCF-7 and MDA-MB-231 cell lines show higher uptake than SKBR-3 between 1 to 8 h of incubation (Fig. 5). However, after 24 h, the internalization amount is the same at all cell lines.

### *Loading of Palbociclib on DcMNPs*

Loading studies of Palbociclib on DcMNPs have been optimized using different buffer solutions (dH2O, PBS, Methanol, TRIS–HCL, and Potassium phosphate) and different generations (3, 3.5, 4, 4.5, 5, 5.5, 7, and 7.5) of DcMNPs. In order to find appropriate DcMNPs generation, the various concentrations of the drug and 2.5 mg/ml of different generations of DcMNPs mixtures were prepared. Solutions were incubated on a rotator for 24, 48, and 72 h at room temperature while protected from light. The nanopar-

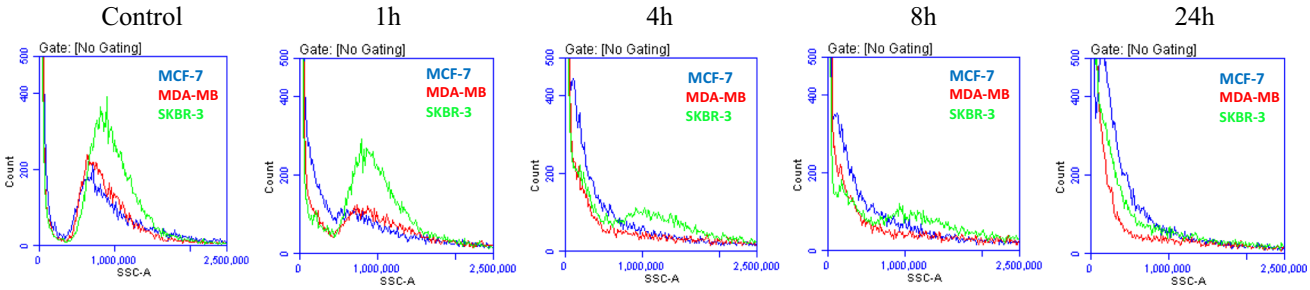


**FIGURE 5. Intensity analysis at different incubation time for MCF-7, MDA-MB-231 and SKBR-3 cell lines.**

ticles loaded with Palbociclib were separated by the magnetic separation method and the absorbance was measured from the supernatant at 218 nm with both a UV spectrophotometer and HPLC methods. By these methods, it was detected that less than 30% of Palbociclib loaded onto different generations of DcMNPs. The data obtained from loading studies showed that Palbociclib was most loaded to DcMNPs in methanol. The nanoparticle generations in which the drug was best loaded were identified as G5 and G5.5. According to the literature, since the terminal carboxyl groups of the G5.5 generation were less toxic than the amine groups in G5, G5.5 nanoparticle generation was selected, and the subsequent studies were continued with this generation.[22]

To find a proper concentration of G5.5 DcMNPs, which the drug was most loaded in methanol, different concentrations of DcMNPs (1–800 $\mu$g/mL) were prepared and all mixed with the same amount (5 $\mu$g/mL) of Palbociclib. The best result was 45% with 500 $\mu$g/mL DcMNPs. To increase the percentage of loading drug to DcMNPs, ultracentrifugal separation method was also used. The same amount of PAMAM-coated MNPs and Palbociclib were mixed for 24 h and then applied to 20,000, 80,000, 100,000, and 150,000$\times g$ ultracentrifugation to increase the precipitation efficiency of the particles. It was observed that 5 $\mu$g/mL Palbociclib was bound to 500 $\mu$g/mL DcMNPs at 100,000$\times g$ with an encapsulation efficacy of 51%. Thus, the loading percentage increased from 45 to 51% after Ultracentrifugation.

### *Conjugation of Palbociclib to DcMNPs*

Since the loading of the drug showed a maximum drug payload of approximately 50%, we tried different conjugation methods to increase the Palbociclib payload on the G5.5 DcMNPs. Several methods were used to prepare the new conjugates. The covalent method for linking the Palbociclib to the PAMAM dendrimer consists of several steps, and we developed a new targeting delivery system for Palbociclib.

Palbociclib (50 $\mu$mol) and EDC were dissolved at DMSO. Succinic acid (SA) was slowly added to the solution, which links Palbociclib and PAMAM dendrimers. Figure 1 illustrates the steps of the synthesis of the PAMAM-drug-PAL conjugate. The HPLC method was used to measure the amount of drug in the supernatant. Using this method, we achieved the highest conjugation efficacy as 75%, so we continued characterization and further experiments by using this method.

Khandare et al. showed that EDC and other carbodiimides could be used for synthesizing biomolecules and their functionalization with other molecules.[15] The ionic bond interaction between Palbociclib and succinic acids causes the preparation of co-amorphous drug systems (Fig. 1). This system improved Palbociclib's solubility, stability and dissolution rate.[31] Furthermore, organic acid-conjugated drugs could bind to OH groups of dendrimers.[15]

The toxicity of SA bound Palbociclib was the same as a free drug in breast cancer cell lines (MCF-7 and MDA-MB-453). Meanwhile, the co-amorphous drug did not have toxic side effects on normal breast cancer cells (MCF-10A) and renal epithelial cells (293 T).[31] Conjugation of the drug by pH-sensitive linker provided the release of the drug after hydrolysis in a tumor acidic environment and after entering the lysosomes. Marcinkowska et al. showed PAMAM- Docetaxel/Paclitaxel conjugates by this method and also showed the toxicity of the drug conjugated nanoparticles in the SKBR-3 and MCF-7 cells. Analyses of cytotoxicity, cellular uptake and internalization of the conjugates by this group suggest that they represent promising vehicles for HER-2-expressing tumor-selective delivery.[20]

### *Characterization of Palbociclib conjugated G5.5 PAMAM DcMNPs*

FTIR, TEM, SEM, and Zeta ($\zeta$) Potential analyses were performed to characterize Palbociclib conjugated G5.5 PAMAM DcMNPs obtained by Conjugation Method.

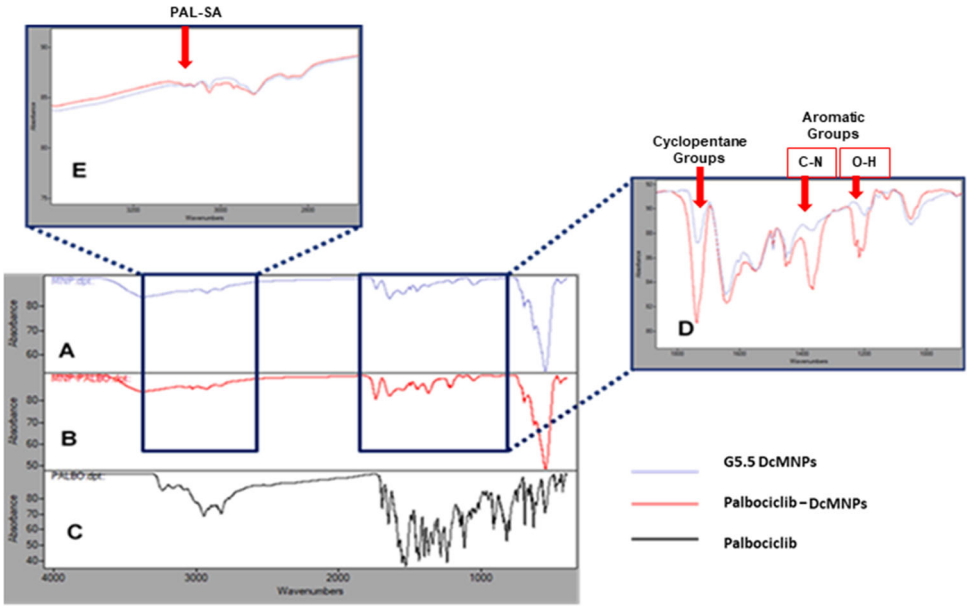


**FIGURE 6. FTIR spectra of (A) Bare G5.5 PAMAM DcMNPs, (B) Palbociclib Conjugated DcMNPs and (C) Free Palbociclib, (D) and (E) Comparison of FTIR Analysis of bare G5.5 PAMAM DcMNPs and Palbociclib conjugated DcMNPs peaks in 1000–1800 and 2000–3200, respectively.**

*Fourier Transform Infrared Spectroscopy (FTIR)*

The FTIR analyses were performed to compare the structures of bare G5.5 PAMAM magnetic nanoparticles, Palbociclib conjugated G5.5 PAMAM magnetic nanoparticles and free Palbociclib (Fig. 6). A significant difference was observed in the FTIR spectrum of bare G5.5 DcMNPs and Palbociclib conjugated DcMNPs between 1180–1250 and 1330–1410 $cm^{-1}$. The 1180–1250 $cm^{-1}$ range indicates the C-O bonds, while the aromatic groups, O–H and C-N bonds, were observed between 1330–1410 $cm^{-1}$.

The peak vibrations between 1700–1820 $cm^{-1}$ show the groups of cyclohexane and cyclopentane. Cyclopentane groups were observed in the Palbociclib conjugated DcMNPs (Fig. 6d). For free Palbociclib, the vibrations of N–H and C-H bonds were observed between 2750–3020 $cm^{-1}$, whereas in Palbociclib conjugated DcMNPs, these bonds were seen between 2800–3080 $cm^{-1}$. Also, PAL-SA had a peak between these ranges at Pal-DcMNPs conjugation (Fig. 6e).[32] Thus these results confirm that Palbociclib was successfully conjugated onto the G5.5 PAMAM DcMNPs.

*Transmission Electron Microscopy and Scanning Electron Microscopy*

The particle shape and size of the G5.5 DcMNPs conjugated with Palbociclib were observed by TEM analysis. According to TEM analysis, the average particle size of the bare G5.5 generation is around 11–13 nm[23] and drug-conjugated nanoparticle dimensions were determined to be 12–14 nm (Figs. 7a and 7b).

SEM images of bare G5.5 PAMAM DcMNPs and Palbociclib conjugated G5.5 DcMNPs indicate the surface properties and size distribution of nanoparticles. According to the results, it was determined that G5.5 PAMAM MNPs showed a homogeneous distribution on the surface and the particle size was approximately 20 nm. The size of the nanoparticles conjugated with the drug was found to be 45 nm (Figs. 7c and 7d).

*Zeta (ζ) Potential*

The zeta potential values of drug conjugated MNPs were measured in deionized water (pH 7.5) with Zetasizer Nano. The data obtained from Zeta Potential Analysis showed that bare G5.5 generation was negatively charged (− 11.6 mV) at neutral pH. This indicates that terminal carboxyl groups are present in the G5.5 generation. Furthermore, the zeta potential of Palbociclib conjugated G5.5 DcMNPs was determined as + 38.2 mV. The conjugation of Palbociclib on G5.5 DcMNPs could explain this significant increase in zeta potential from − 11.6 to + 38.2 mV and neutralization of the negative charge on the nanoparticle surface.

The zeta potential indicates the degree of repulsion between adjacent, similarly charged particles in the dispersion. For particles that are small enough, a high zeta potential will confer stability, i.e., the solution or dispersion will resist aggregation. Conversely, when the zeta potential is low, attraction exceeds repulsion

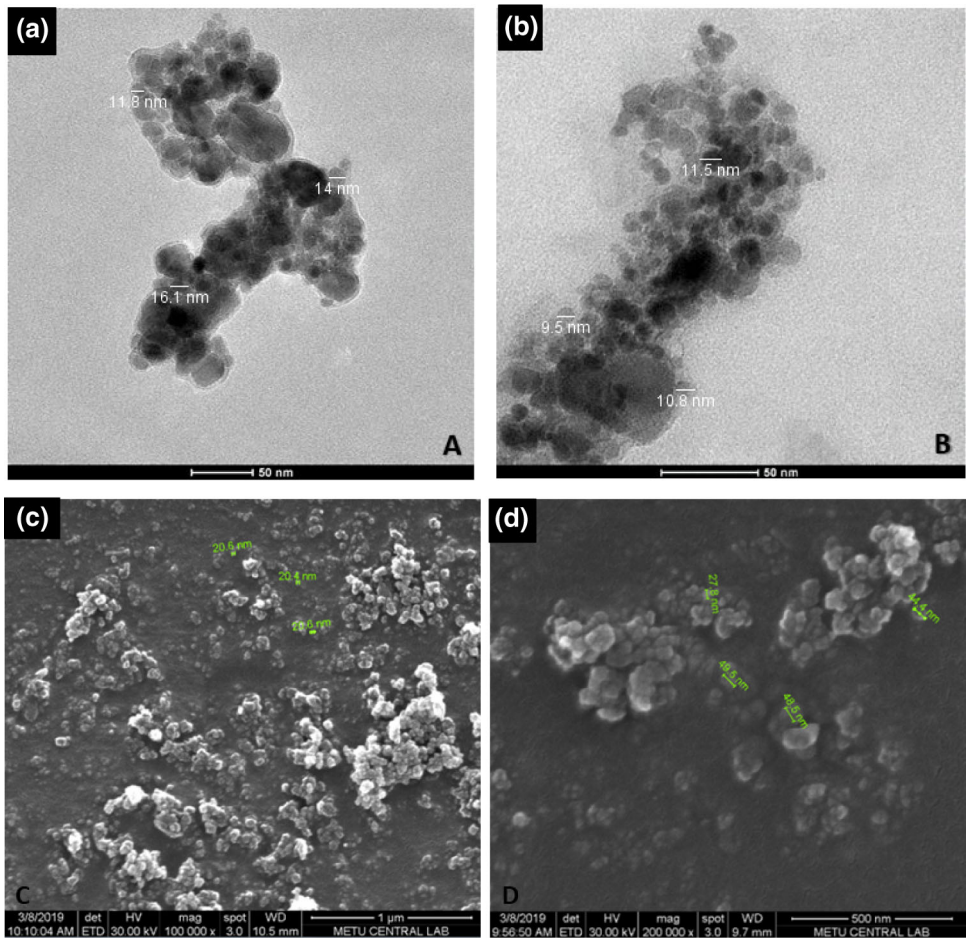


**FIGURE 7. TEM images of (a) bare G5.5 PAMAM DcMNPs and (b) Palbociclib conjugated G5.5 PAMAM DcMNPs. SEM images of (c) bare G5.5 DcMNPs and (d) Palbociclib conjugated G5.5 DcMNPs.**

and the dispersion will break and flocculate. So, colloids with high zeta potential (negative or positive) are electrically stabilized, while colloids with low zeta-potentials tend to coagulate or flocculate.[27]

### *LDH Cytotoxicity Assay*

LDH release assay was used for cytotoxicity analysis. Measurements were made at 24, 48, 72, and 96 h of incubation. The release of LDH into the medium demonstrated cell death.[14] It is possible to distinguish between cell death and growth inhibition using an LDH cytotoxicity assay based on modified LDH.[25] When a cell loses membrane integrity, it releases LDH, which is then used as a catalyst to promote a two-step reaction. The first step is the oxidation–reduction reaction between $NAD^+$ and lactate. This is followed by the reduction of a tetrazolium salt (INT) to a colored formazan. The colored formazan product can be detected colorimetrically through the absorbance maximum at 450–520 nm.

The G5.5 PAMAM dendrimer was conjugated to Palbociclib by the pH-depended linker. This drug conjugation method is stable in extracellular media.[20] The carboxyl-terminal dendrimer is transported to the cell by an absorptive endocytosis mechanism.[15] The drug is released in the acidic environment of the lysosome.

The responses of all cell lines to the increasing concentration of Palbociclib and PAL-DcMNPs are shown in Fig. 8. The results showed the rising release of LDH due to the treatment of PAL-DcMNPs after 96 h. However, no significant LDH release was seen due to treatment with an increasing concentration of bare DcMNPs (the same amount as PAL-DcMNPs) at 96 h.

### *Cell Viability Assay*

The determination of ATP production is a method to analyze cellular viability in anticancer studies. In this study, the CellTiter-Glo® Cell Viability Assay is used to determine the number of viable cells in cell

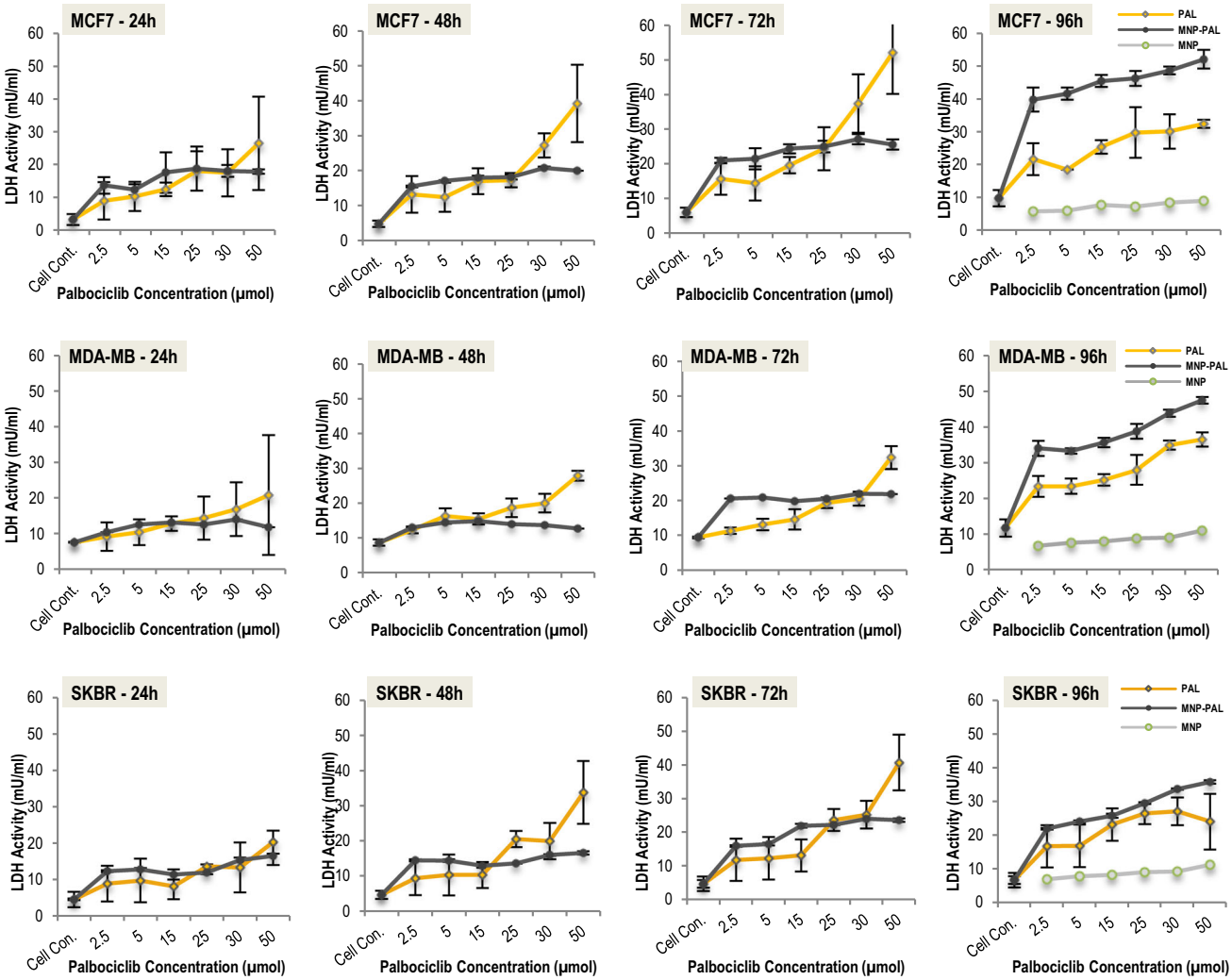


**FIGURE 8. LDH activity of Palbociclib, PAL-DcMNPs and bare DcMNPs on (a) MCF-7, (b) MDA-MB-231, (c) SKBR-3.**

culture after 96 treatments with Palbociclib and PAL-DcMNPs. The metabolic activity of the cell was measured by the production of ATP, and it is based on the conversion of luciferase into oxyluciferin in an ATP-dependent reaction that generates light. Thus, the level of ATP correlates with the amount of light emission. Cell viability can then be correlated to an increase in the overall amount of ATP produced in a population of exponentially growing cells. This assay is particularly useful because it is sensitive enough to reproducibly detect ATP production from a single mammalian cell. An additional benefit is the extended dynamic range of this assay, as a concentration of ATP and cellular viability are directly proportional to cell numbers between one and one hundred million cells.

The cytotoxicity of Palbociclib and PAL-DcMNPs were dose-dependent (Fig. 9). At the higher concentrations (30–50 $\mu$M), free Palbociclib has a more cytotoxic effect on MCF-7, MDA-MB-231, and SKBR-3 breast cancer cell lines. However, with Palbociclib conjugated DcMNPs treatment, it has been observed that drug doses that inhibit 50% of the cell viability can be achieved with even lower drug concentrations with respect to free Palbociclib for all of the breast cancer cell lines. These results show that conjugation of Palbociclib with DcMNPs improved the cytotoxic effect in lower drug concentrations. The observed effects were more evident for MCF-7 cells than for MDA-MB231 and SKBR3 cells. In addition, the association between cell viability data and LDH release was also observed at a lower dosage of PAL-DcMNPs. The values of LDH are relatively high, considering that viability decreased to 30% at 2.5 $\mu$M treatment of PAL-DcMNPs at MCF-7 cells.

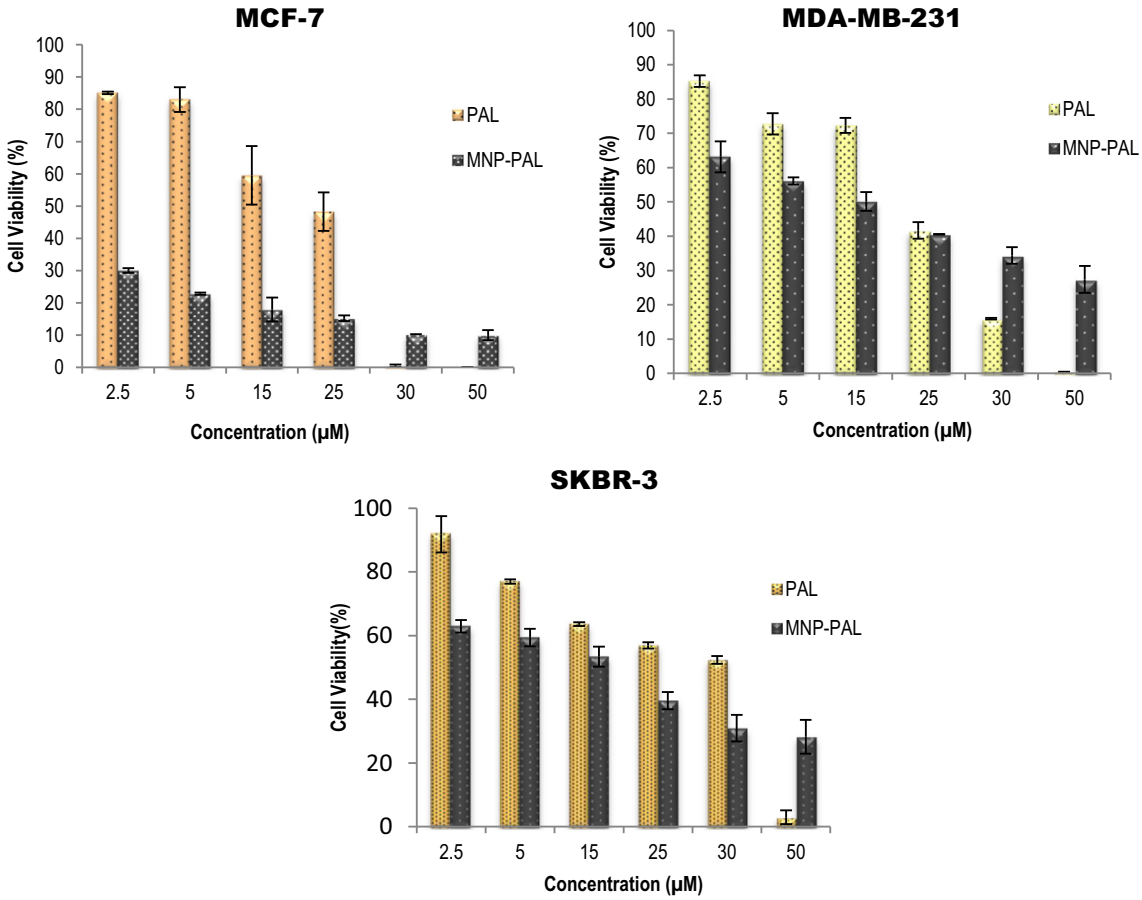


**FIGURE 9. CellTiter-Glo® Cell Viability Assay (a) MCF-7, (b) MDA-MB-231, and (c) SKBR-3 cell lines.**

*Quantification of the expression level of Bax, Bcl-2, CDH1, MDR1, and mTOR Genes in Untreated and Treated Breast Cancer Cells*

To elucidate the difference in apoptotic status between untreated and treated breast cancer cells, the expression pattern of the genes related to apoptosis (Bax, Bcl-2), migration (CDH1), drug resistance (MDR1), and cell proliferation (mTOR), in MDA-MB231, SKBR3, and MCF7 cell lines was examined by qRT-PCR before and after treatment of the cells with 15 $\mu$M Palbociclib, bare G5.5 PAMAM DcMNPs, and Pal-DcMNPs for 96 h.

Apoptosis is the orderly and tightly regulated cellular programmed cell death involving signal transduction pathways that induce cells to self-destruct during embryonic development or in response to environmental hazards or anticancer therapeutics. In evaluation of expression analysis of Bcl-2 and Bax, the ratio of pro-apoptotic Bax to anti-apoptotic Bcl-2 expression was considered as an apoptotic parameter.[30] According to Fig. 10, Bax/Bcl-2 ratio increased, followed by Pal-DcMNPs stimulation at the mRNA level in all three cell lines, MDA-MB231, SKBR3, and MCF7. Increased ratio might be correlated to decreased cell viability of these cell lines after treatment with Pal-DcMNPs. These results could validate our data obtained from the cell viability analysis, which showed that treating with Pal-DcMNPs causes cell death in the breast cancer cell lines.

CDH1 (E-cadherin) is considered as a calcium-dependent transmembrane protein that facilitates the assembly of the specialized intercellular junctions required for the adherence of epithelial cells.[24, 29] According to various *in vitro* experiments, CDH1 expression is downregulated in colon cancer cell lines which leads to cell migration and invasion.[18] Other studies have indicated that loss of CDH1 expression is related to the metastasis of lymph nodes,[6, 12, 17] distant metastasis, and increased mortality.[6, 12]

The results of our study revealed that the CDH1 gene was significantly upregulated in all the treatment groups, in comparison to the untreated control group (Fig. 11). However, the rise of CDH1 expression was higher in the case of Pal-DcMNPs treated cell lines. Combined with the findings of previous studies, it can be said that CDH1 may participate in the Pal-

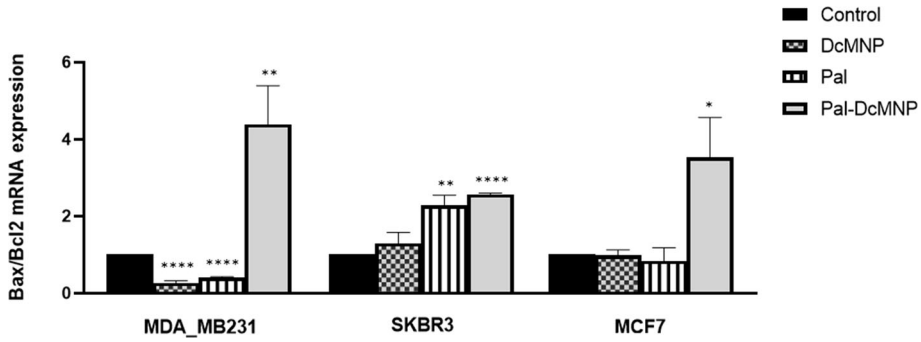


**FIGURE 10. Expression levels of Bax and Bcl-2 genes in untreated and treated MDA-MB231, SKBR3, and MCF7 cell lines with 15 $\mu$M Palbociclib, bare G5.5 PAMAM DcMNPs, and Pal-DcMNPs for 96 h, when $p < 0.05$.**

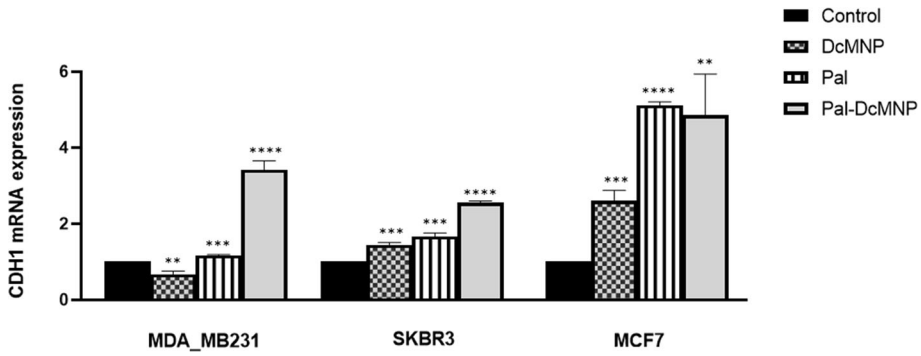


**FIGURE 11. Expression levels of CDH1 gene in untreated and treated MDA-MB231, SKBR3, and MCF7 cell lines with 15uM Palbociclib, bare G5.5 PAMAM DcMNPs, and Pal-DcMNPs for 96 h, when $p < 0.05$.**

DcMNPs-mediated inhibition of cell proliferation and metastasis.

In literature, there are some data indicating the involvement of Cdh1 in apoptotic cell death which is initially reported in B-lymphoma and also, overexpression of Cdh1 can dramatically cause cell susceptibility to natural killer cell (NK) cytotoxicity.[12] Regarding these results, there could be a possible association between CDH1 overexpression and decreased cell viability in MDA-MB231, SKBR3, and MCF7 cell lines after treating with Pal-DcMNPs in our study.

P-glycoprotein 1 (multidrug resistance protein 1, MDR1), is considered as an important cell membrane protein which pumps out many foreign substances from the cells. Consequently, overexpression of P-gp is related to the main mechanism leading to decreasing intracellular drug accumulation and developing of multidrug resistance in human multidrug-resistant (MDR) cancers. According to the results of our study, we found that after treatment with Palbociclib conjugated DcMNPs, MDR1 gene expression levels did not significantly change in MDA-MB231 and MCF7 cell lines (Fig. 12). However, in SKBR3 cells, a statistically significant decrease was observed in Palbociclib-conjugated DcMNPs cells compared to untreated cells ($p < 0.05$), and it was not altered when treated with Palbociclib and DcMNPs alone, suggesting that this chemotherapeutic drug can decrease the mRNA expression of the MDR1 gene when conjugated with DcMNPs. Our results in MCF7 cells are in consistent with the study performed by Chen et al. (Everolimus Reverses Palbociclib Resistance in ER+ Human Breast Cancer Cells by Inhibiting Phosphatidylinositol 3-Kinase (PI3K)/Akt/Mammalian Target of Rapamycin (mTOR) Pathway), which indicated that there is no significant change in MDR1 gene expression either in mRNA or in protein level in Palbociclib-treated MCF7 cell line.

It is well known that mTOR is one of the Phosphoinositide 3-kinase (PI3K) downstream molecules which regulates cell proliferation, apoptosis and autophagy.[32] According to the studies, an increase in tumor progression and often a decrease in patient survival is indicated followed by mTOR signaling activation.[8] The activity of mTOR is frequently upregulated in human cancer.[9] In a study, noncanonical downregulation of mTOR by Palbociclib treatment was indicated in patient-derived SF7761 and SF8628 glioma cell lines and it was shown that combined used of CDK4/6 and mTOR inhibitors induce synergistic growth arrest.[3] Another study recently

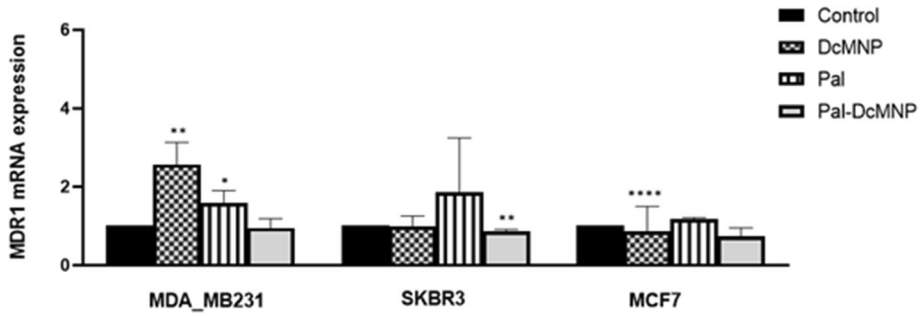


**FIGURE 12. Expression levels of MDR1 gene in untreated and treated MDA-MB231, SKBR3, and MCF7 cell lines with 15 $\mu$M Palbociclib, bare G5.5 PAMAM DcMNPs, and Pal-DcMNPs for 96 h, when $p < 0.05$.**

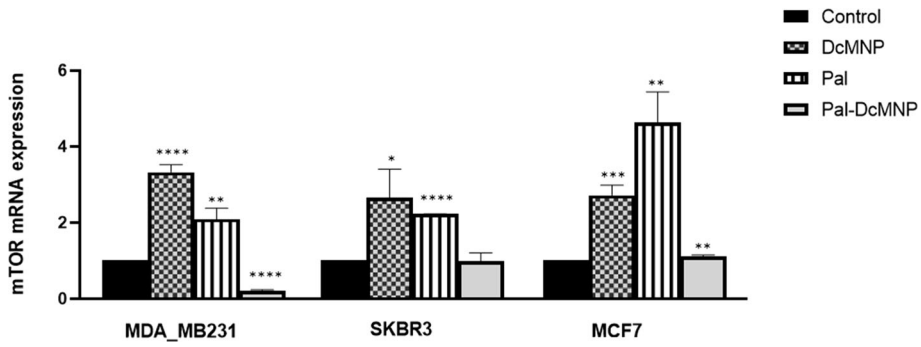


**FIGURE 13. Expression levels of mTOR gene in untreated and treated MDA-MB231, SKBR3, and MCF7 cell lines with 15 $\mu$M Palbociclib, bare G5.5 PAMAM DcMNPs, and Pal-DcMNPs for 96 h, when $p < 0.05$.**

reported that Palbociclib treatment increases the activation of AKT/mTOR signaling.[4, 33] In our study, it can be seen an upregulation in the expression of mTOR in MDA-MB231, SKBR3, and MCF7 cell lines treated with free Palbociclib (Fig. 13). These results are in consistent with the data obtained from the study performed by Cretella et al., in which Palbociclib induced a dose-dependent up-regulation of the phosphorylation levels of mTOR protein and its activation in MDA-MB231 and HCC38 cells.[5] Our results indicated upregulation of mTOR after treatment with Palbociclib conjugated DcMNPs in MCF7 cell line. However, downregulation of mTOR in MDA-MB231 cell line by Palbociclib conjugated DcMNPs treatment was indicated in our data obtained from qRT-PCR assay. In SKBR-3 cell line, no change has been seen after treating by Pal- DcMNPs.

## CONCLUSIONS

DcMNPs maintain a suitable drug delivery system due to their surface functional groups, small sizes, and targeting ability under the magnetic field. The present study presents many loading and conjugation methods that indicate different amounts of Palbociclib with various generations of PAMAM dendrimers. According to the HPLC and characterization results, the most efficient Palbociclib conjugation to magnetic PAMAM dendrimers was approximately 75 percent. The synthesized PAL-DcMNPs have a high potential to be used as a tumor-targeting and pH-responsive drug delivery system due to pH-sensitive linkers. Therefore, it can be an efficient system to reduce the side effects of drugs and also eliminate drug resistance in cancer cells. It has been observed that PAL-DcMNPs treatment can inhibit 50% of the cell viability even in lower drug concentrations in the MCF-7, MDA-MB-231, and SKBR3 breast cancer cell lines. This effect may be by regulating the expression of apoptosis- and drug resistance-related genes. Thus, PAL- DcMNPs may be a potential candidate as a therapeutic agent for breast cancer, considering their ability to stimulate apoptosis which may inhibit the growth of cancer cells.

## ACKNOWLEDGMENTS

This study was supported by The Scientific and Technological Research Council of Turkey (TUBITAK 1001 Project No.117Z092).

## CONFLICT OF INTEREST

The authors declare that they have no conflict of interest.

## REFERENCES


[1]Arruebo, M., et al. Magnetic nanoparticles for drug delivery. *Nano Today*. 2(3):22–32, 2007.

[2]Arya, G., et al. 'Enhanced antiproliferative activity of Herceptin (HER2)-conjugated gemcitabine-loaded chitosan nanoparticle in pancreatic cancer therapy. *Nanomed. Nanotechnol. Biol. Med.* 7(6):859–70, 2011. https://doi.org/10.1016/j.nano.2011.03.009.

[3]Asby, D. J., et al. Combined use of CDK4/6 and mTOR inhibitors induce synergistic growth arrest of diffuse intrinsic pontine glioma cells via mutual downregulation of mTORC1 activity. *Cancer Manag. Res.* 10:3483–3500, 2018. https://doi.org/10.2147/CMAR.S167095.

[4]Bonelli, M. A., et al. Combined inhibition of CDK4/6 and PI3K/AKT/mTOR pathways induces a synergistic anti-tumor effect in malignant pleural mesothelioma cells. *Neoplasia (United States)*. 19(8):637–648, 2017. https://doi.org/10.1016/j.neo.2017.05.003.

[5]Cretella, D., et al. The anti-tumor efficacy of CDK4/6 inhibition is enhanced by the combination with PI3K/AKT/mTOR inhibitors through impairment of glucose metabolism in TNBC cells. *J. Exp. Clin. Cancer Res.* 37(1):1–12, 2018. https://doi.org/10.1186/s13046-018-0741-3.

[6]Filiz, A. I., et al. The survival effect of E-cadherin and catenins in colorectal carcinomas. *Colorectal Dis.* 12(12):1223–1230, 2010. https://doi.org/10.1111/j.1463-1318.2009.01994.x.

[7]Gupta, A. K., et al. Palbociclib: a breakthrough in breast carcinoma in women. *Med. J Armed Forces India*. 72:S37–S42, 2016. https://doi.org/10.1016/j.mjafi.2015.11.002.

[8]Hare, S. H., and A. J. Harvey. mTOR function and therapeutic targeting in breast cancer. *Am. J. Cancer Res.* 7(3):383–404, 2017.

[9]Hua, H., et al. 'Targeting mTOR for cancer therapy. *J. Hematol. Oncol.* 12(1):1–19, 2019. https://doi.org/10.1186/s13045-019-0754-1.

[10]Jain, A., et al. Dendrimer: a complete drug carrier. *Int. J. Pharm. Sci. Res.* 1(4):38–52, 2010.

[11]Jiang, Y., et al. PEGylated PAMAM dendrimers as a potential drug delivery carrier: in vitro and in vivo comparative evaluation of covalently conjugated drug and noncovalent drug inclusion complex. *J. Drug Target.* 18(5):389–403, 2010. https://doi.org/10.3109/10611860903494203.

[12]Jie, D., et al. Positive expression of LSD1 and negative expression of E-cadherin correlate with metastasis and poor prognosis of colon cancer. *Digest. Dis. Sci.* 58(6):1581–1589, 2013. https://doi.org/10.1007/s10620-012-2552-2.

[13]Jochums, A., et al. Revelation of different nanoparticle-uptake behavior in two standard cell lines NIH/3T3 and A549 by flow cytometry and time-lapse imaging. *Toxics*. 5(3):15, 2017. https://doi.org/10.3390/toxics5030015.

[14]Kaja, Simon, et al. An optimized lactate dehydrogenase release assay for screening of drug candidates in neuroscience. *J. Pharmacol. Toxicol. Methods*. 2016. https://doi.org/10.1016/j.vascn.2015.02.001.

[15]Khandare, J., et al. Synthesis, cellular transport, and activity of polyamidoamine dendrimer-methylprednisolone conjugates. *Bioconjug. Chem.* 16(2):330–337, 2005. https://doi.org/10.1021/bc0498018.

[16]Khodadust, R., et al. PAMAM dendrimer-coated iron oxide nanoparticles: synthesis and characterization of different generations. *J. Nanopart. Res.* 15(3):1488, 2013. https://doi.org/10.1007/s11051-013-1488-6.

[17]Kwak, J. M., et al. The prognostic significance of E-cadherin and liver intestine-cadherin expression in colorectal cancer. *Dis. Colon Rectum*. 50(11):1873–1880, 2007. https://doi.org/10.1007/s10350-007-9034-1.

[18]Lu, M. H., et al. Prospero homeobox 1 promotes epithelial-mesenchymal transition in colon cancer cells by inhibiting e-cadherin via miR-9. *Clin. Cancer Res.* 18(23):6416–6425, 2012. https://doi.org/10.1158/1078-0432.CCR-12-0832.

[19]Marcinkowska, M., et al. Conjugate of PAMAM dendrimer, doxorubicin and monoclonal antibody-trastuzumab: the new approach of a well-known strategy. *Polymers*. 10(2):1–11, 2018. https://doi.org/10.3390/polym10020187.

[20]Marcinkowska, M., et al. Multicomponent conjugates of anticancer drugs and monoclonal antibody with PAMAM dendrimers to increase efficacy of HER-2 positive breast cancer therapy. *Pharm. Res.* 2019. https://doi.org/10.1007/s11095-019-2683-7.

[21]Parsian, M., et al. Characterization of gemcitabine loaded polyhydroxybutyrate coated magnetic nanoparticles for targeted drug delivery. *Anti-Cancer Agents Med. Chem.* 20:1–8, 2020. https://doi.org/10.2174/1871520620666200310091026.

[22]Parsian, M., P. Mutlu, et al. Half generations magnetic PAMAM dendrimers as an effective system for targeted gemcitabine delivery. *Int. J. Pharm.* 515(1–2):104–113, 2016. https://doi.org/10.1016/j.ijpharm.2016.10.015.

[23]Parsian, M., G. Unsoy, et al. 'Loading of Gemcitabine on chitosan magnetic nanoparticles increases the anti-cancer efficacy of the drug. *Eur. J. Pharmacol.* 784:121–128, 2016. https://doi.org/10.1016/j.ejphar.2016.05.016.

[24]Qian, Z. R., et al. Tumor-specific downregulation and methylation of the CDH13 (H-cadherin) and CDH1 (E-cadherin) genes correlate with aggressiveness of human pituitary adenomas. *Mod. Pathol.* 20(12):1269–1277, 2007. https://doi.org/10.1038/modpathol.3800965.

[25]Smith, S. M., et al. A simple protocol for using a LDH-Based cytotoxicity assay to assess the effects of death and growth inhibition at the same time. *PLoS ONE*. 2011. https://doi.org/10.1371/journal.pone.0026908.

[26]Taghavi Pourianazar, N., et al. Bioapplications of poly(amidoamine) (PAMAM) dendrimers in nanomedicine. *J. Nanopart. Res.* 16(4):2342, 2014. https://doi.org/10.1007/s11051-014-2342-1.

[27]Taghavi Pourianazar, N., et al. 'CpG oligodeoxynucleotide-loaded PAMAM dendrimer-coated magnetic nanoparticles promote apoptosis in breast cancer cells. *Biomed. Pharmacother.* 78:81–91, 2016. https://doi.org/10.1016/j.biopha.2016.01.002.

[28]Teirlinck, E., et al. Exploring light-sensitive nanocarriers for simultaneous triggered antibiotic release and disruption of biofilms upon generation of laser-induced vapor nanobubbles. *Pharmaceutics*. 11(5):201, 2019. https://doi.org/10.3390/pharmaceutics11050201.

[29]Tsanou, E., et al. The E-cadherin adhesion molecule and colorectal cancer. A global literature approach. *Anticancer Res.* 28(6):3815–3826, 2008.
[30]Zapata, J. M., et al. Expression of multiple apoptosis-regulatory genes in human breast cancer cell lines and primary tumors. *Breast Cancer Res. Treat.* 47(2):129–140, 1998. https://doi.org/10.1023/A:1005940832123.
[31]Zhang, J., et al. Inhibition of Rb phosphorylation leads to mTORC2-mediated activation of Akt. *Mol. Cell.* 62(6):929–942, 2017. https://doi.org/10.1016/j.molcel.2016.04.023.
[32]Zhang, H. W., et al. Flavonoids inhibit cell proliferation and induce apoptosis and autophagy through downregulation of PI3K$\gamma$ mediated PI3K/AKT/mTOR/p70S6K/ULK signaling pathway in human breast cancer cells. *Sci. Rep.* 8(1):1–13, 2018. https://doi.org/10.1038/s41598-018-29308-7.
[33]Zhang, M., et al. Co-amorphous palbociclib-organic acid systems with increased dissolution rate, enhanced physical stability and equivalent biosafety. *RSC Adv.* 9(7):3946–3955, 2019. https://doi.org/10.1039/c8ra09710k.